

ms2: A molecular simulation tool for thermodynamic properties, release 3.0

Gábor Rutkai^a, Andreas Köster^a, Gabriela Guevara-Carrion^a, Tatjana Janzen^a, Michael Schappals^b, Colin W. Glass^c, Martin Bernreuther^c, Amer Wafai^c, Simon Stephan^b, Maximilian Kohns^b, Steffen Reiser^b, Stephan Deublein^b, Martin Horsch^b, Hans Hasse^b, Jadran Vrabec^{a,*}

^a*Lehrstuhl für Thermodynamik und Energietechnik, Universität Paderborn, 33098 Paderborn, Germany*

^b*Lehrstuhl für Thermodynamik, Universität Kaiserslautern, 67653 Kaiserslautern, Germany*

^c*Höchstleistungsrechenzentrum Universität Stuttgart (HLRS), 70550 Stuttgart, Germany*

Abstract

A new version release (3.0) of the molecular simulation tool *ms2* [Deublein et al., Comput. Phys. Commun. 182 (2011) 2350 and Glass et al., Comput. Phys. Commun. 185 (2014) 3302] is presented. Version 3.0 of *ms2* features two additional ensembles, i.e. microcanonical (*NVE*) and isobaric–isoenthalpic (*NpH*), various Helmholtz energy derivatives in the *NVE* ensemble, thermodynamic integration as a method for calculating the chemical potential, the six Maxwell-Stefan diffusion coefficients of quaternary mixtures, statistics for sampling hydrogen bonds, the osmotic pressure for calculating the activity of solvents, smooth-particle mesh Ewald summation as well as the ability to carry out molecular dynamics runs for an arbitrary number of state points in a single program execution.

Keywords: molecular simulation, molecular dynamics, Monte Carlo

New version program summary

Program Title: *ms2*

Operating system: Unix/Linux

Licensing provisions: Special license supplied by the authors

Programming language: Fortran95

Has the code been vectorized or parallelized: yes (Message Passing Interface (MPI) protocol and OpenMP)

*Corresponding author: Jadran Vrabec, Warburger Str. 100, 33098 Paderborn, Germany, Tel.: +49-5251/60-2420, Email: jadran.vrabec@upb.de

Distribution format: tar.gz

Classification: 7.7, 7.9, 12

Catalogue identifiers of previous versions: AEJF_v1_0 and AEJF_v2_0

Supplementary material: A detailed description of the parameter setup for thermodynamic integration and hydrogen bonding is given in the supplementary material. Furthermore, all molecular force field models developed by our group are provided

Journal reference of previous versions: Deublein et al., Comput. Phys. Commun. 182 (2011) 2350 and Glass et al., Comput. Phys. Commun. 185 (2014) 3302

Does the new version supersede the previous version?: Yes

Reasons for the new version: Introduction of new features as well as enhancement of computational efficiency

Summary of revisions: Two new ensembles (NVE and NpH), new properties (Helmholtz energy derivatives, chemical potential via thermodynamic integration, Maxwell-Stefan diffusion coefficients of quaternary mixtures, activity coefficients via osmotic pressure), new functionalities (detection and statistics of hydrogen bonding, smooth-particle mesh Ewald summation, ability to carry out molecular dynamics runs for an arbitrary number of state points in a single program execution)

Nature of problem: Calculation of application oriented thermodynamic properties: vapor-liquid equilibria of pure fluids and multi-component mixtures, thermal, caloric and entropic data as well as transport properties

Solution method: Molecular dynamics, Monte Carlo, various ensembles, Grand Equilibrium method, Green-Kubo formalism, Lustig formalism, OPAS method, smooth-particle mesh Ewald summation

Typical running time: Typically from a couple of hours up to days, depending on the specific scenario (system size, calculated properties, number of CPU cores used)

Restrictions: Typical problems addressed by *ms2* are solved by simulating systems containing 1000 to 5000 molecules that are modelled as rigid bodies

Documentation: Documentation is provided with the installation package and is available at <http://www.ms-2.de>

1. Introduction

Due to the continuous increase in computing power, the range of possible applications of molecular modeling and simulation has become broader over time, proceeding from qualitative basic research in soft matter physics to quantitative applications in chemical engineering. Reaching agreement with the available experimental data, and predicting properties where experimental data are rare or absent, molecular methods transform engineering data science [1, 2]. This progress is driven by massively-parallel high performance computing with scalable codes [3] and by the concurrent execution of large numbers of simulations [4] or of simulations which can be decomposed into a large number of concurrent tasks [5–7].

The program *ms2* (molecular simulation 2) was designed to compute thermodynamic properties of pure fluids and mixtures by Monte Carlo (MC) and molecular dynamics (MD) simulation. Licences are available without cost for all purposes which concern academic research and teaching [8]. The previous two major releases of *ms2* [9, 10] facilitate the simulation of vapor-liquid equilibria (VLE) by Grand Equilibrium simulation and the computation of many thermodynamic bulk properties, including linear transport coefficients, for molecular models consisting of Lennard-Jones interaction sites, point charges and point multipoles. It has been shown that such models can reach a high accuracy for a wide variety of thermodynamic properties for many molecular fluids [11–16], leading to an increasing popularity of molecular methods in the engineering sciences [17–21].

Similar molecular simulation programs, which address multiple academic communities, include CHARMM [22], DL_POLY [23], ESPResSo [24], GIBBS [25], GROMACS [26], IMD [27], LAMMPS [28], *ls1* mardyn [29], NAMD [30], TINKER [31] and Towhee [32]. In comparison with these codes, the aim of *ms2* is to focus on applications of molecular modeling and simulation in fluid process engineering, both industrial and academic. Hence, a high accuracy, short response times and the suitability for coupling with equations of state [4, 33] and rigorous model optimization approaches [34–36] have been priorities in developing both the code base as well as the toolset which is provided jointly with it. The present work discusses the third major release of *ms2* and its most important innovations, which are presented in detail in the following sections.

2. Microcanonical and isobaric-isoenthalpic ensembles

An ensemble is the set of all theoretically possible microscopic configurations on the molecular level under specific macroscopic constraints. The microcanonical (NVE) ensemble is the set of all configurations that fulfill the condition of having the same number of particles N , volume V and energy E , whereas the isobaric-isoenthalpic (NpH) ensemble represents a system at constant number of particles N , pressure p and enthalpy H . Molecular dynamics (MD) mimics the time evolution of a mechanical system by numerically solving Newton’s equations of motion for all considered molecules. Because of the nature of this solution, the time is discretized and the method yields microscopic configurations at discrete and consecutive time steps. The Monte Carlo (MC) method is the application of statistical mechanics to describe molecular systems. With this approach, microscopic configurations are generated by random numbers that are potentially accepted such that only relevant and physically meaningful configurations are sampled [37]. The generation and acceptance of these configurations is governed by specific probabilities that are ensemble-dependent

Table 1: Comparison of the ensembles implemented in *ms2* for methyl fluoride [41] in terms of temperature T , density ρ , pressure p and potential energy u . Numbers in parentheses denote statistical uncertainties in the last digit that were estimated with the block averaging method of Flyvbjerg and Petersen [42].

		T	ρ	p	u
		K	mol/l	MPa	kJ/mol
MD	<i>NVT</i>	300	1	2.090(2)	-1048(3)
	<i>NpT</i>	300	1.0015(7)	2.090	-1051(3)
	<i>NVE</i>	300.0(1)	1	2.088(1)	-1048(3)
	<i>NpH</i>	300.0(1)	1.0003(2)	2.090	-1048(2)
MC	<i>NVT</i>	300	1	2.0880(2)	-1051.6(2)
	<i>NpT</i>	300	1.0019(2)	2.0880	-1053.6(3)
	<i>NVE</i>	299.99(1)	1	2.0882(2)	-1051.3(2)
	<i>NpH</i>	300.06(2)	1.0010(1)	2.0880	-1051.7(2)

and described in the literature for essentially every relevant ensemble. For MC simulations, the *NVE* and *NpH* ensembles were implemented in *ms2* release 3.0 according to Refs. [38, 39]. For MD simulations, the pressure is kept constant using Andersen’s barostat [40] in case of the *NpH* ensemble. Because the solution of Newton’s equations of motion is approximate, the total energy of the system $E = K + U$, which consists of a kinetic K (exclusively molecular momentum dependent) and potential U (exclusively molecular position dependent) energy contribution, is not rigorously conserved in a standard MD run mainly for numerical reasons. Therefore, the translational and rotational momentum of every molecule is rescaled such that the total kinetic energy K fulfils $K = E - U$, where the total energy E is specified and the potential energy U is calculated from the current microscopic configuration. For a *NpH* ensemble run, the solution is analogous: Momenta are rescaled such that the current kinetic energy K fulfils $K = H - U - pV$, where H and p are specified, U and V are dependent on the current microscopic configuration. This extends the ensembles available in *ms2* to five: *NVT*, *NVE*, *NpT*, *NpH* and μVT , where μ is the chemical potential.

For verification purposes, Table 1 contains numerical results for methyl fluoride modeled by a quadrupolar two-center Lennard–Jones potential [41] at $T = 300$ K and $\rho = 1$ mol/l. Figure 1 shows the running averages of the calculated properties in Table 1 at the same state point.

3. Helmholtz energy derivatives in the microcanonical ensemble

The generalized calculation of the Helmholtz energy derivatives

$$A_{nm}^r = (1/T)^n \rho^m \frac{\partial^{n+m} f^r(T, \rho) / (RT)}{\partial (1/T)^n \partial \rho^m}, \quad (1)$$

with the molar residual Helmholtz energy f^r , the temperature T , the density ρ and the molar gas constant R was introduced in *ms2* also for the *NVE* ensemble up to the order $n = 3$ and

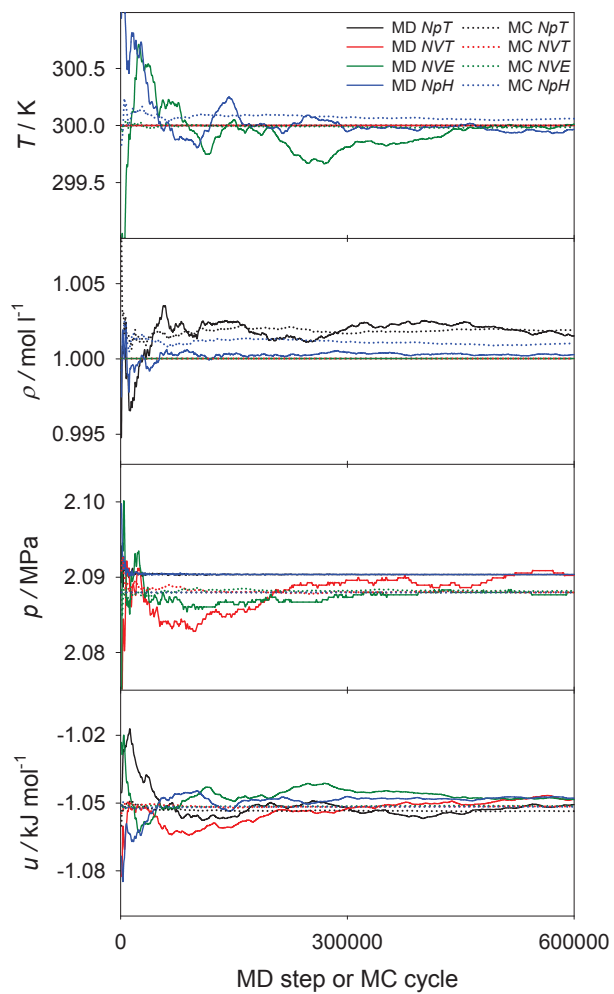


Figure 1: Comparison of the ensembles implemented in *ms2* for methyl fluoride [41] in terms of running averages for temperature T , density ρ , pressure p and potential energy u .

Table 2: Comparison of the residual Helmholtz energy derivatives A_{nm}^r of methyl fluoride [41] at $T = 300$ K and $\rho = 1$ mol/l. Numbers in brackets denote statistical uncertainties in the last digit that were estimated with the block averaging method of Flyvbjerg and Petersen [42]. Superscripts (1) and (2) indicate the two different entropy definitions [45].

		A_{10}^r	A_{01}^r	A_{20}^r	A_{11}^r	A_{02}^r
MD	<i>NVT</i>	-0.420(1)	-0.1620(6)	-0.54(4)	-0.40(2)	0.03(3)
	<i>NVE</i> ¹	-0.418(1)	-0.1622(4)	-0.55(3)	-0.37(1)	0.05(3)
	<i>NVE</i> ²	-0.418(1)	-0.1621(4)	-0.55(3)	-0.37(1)	0.05(3)
MC	<i>NVT</i>	-0.42158(8)	-0.16290(8)	-0.562(2)	-0.391(2)	0.011(6)
	<i>NVE</i> ¹	-0.42149(5)	-0.16280(8)	-0.560(2)	-0.385(3)	0.024(6)
	<i>NVE</i> ²	-0.42133(5)	-0.16274(8)	-0.560(2)	-0.385(3)	0.024(6)

$m = 2$. The total reduced Helmholtz energy $f/(RT)$ can be additively separated into an ideal $f^o/(RT)$ and a residual contribution $f^r/(RT)$. The ideal contribution by definition corresponds to the value of $f/(RT)$ when no intermolecular interactions are at work [43]. $f^o/(RT)$ consists of an exclusively temperature and an exclusively density dependent part. The latter is the trivial term $\ln(\rho/\rho_{\text{ref}})$, whereas the former is non-trivial. A formalism that allows for the calculation of the residual Helmholtz derivatives on the fly from a single simulation run per state point was published by Lustig [44, 45] and was already introduced for the *NVT* ensemble in the preceding program version. *ms2* release 3.0 now yields these derivatives also for the *NVE* ensemble. However, in contrast to *NVT* simulations, there are two numerical results for each calculated derivative A_{nm} due to the two possible entropy definitions in statistical mechanics [45]. In any case, these two different sets of results must be identical in the thermodynamic limit ($N \rightarrow \infty$). In practice, they already agree within their statistical uncertainty for a simulation based on around a thousand molecules. For verification purposes, Table 2 contains numerical results for methyl fluoride [41]. A detailed description of the calculation of these derivatives can be found in Ref. [45]. Their conversion into common thermodynamic properties is provided in the supplementary material of release 2.0 of *ms2* [10] and in Ref. [43].

4. Thermodynamic integration

The previously described method of Lustig does not allow for the direct sampling of the chemical potential and other entropic properties like A_{00}^r . Such an effort requires techniques based on free energy calculation, such as particle insertion and/or thermodynamic integration [37]. Widom’s particle insertion method [46] is a conceptually straightforward approach to calculate the chemical potential with a low computational cost, both for pure substances and mixtures. The total chemical potential μ_i of species i can be separated into an ideal (o) and a residual (r) contribution in the same way as the Helmholtz energy is decomposed, cf. section 2: $\mu_i(T, \rho, x_i) = \mu_i^o(T) + RT \ln(N_i/(V\rho_{\text{ref}})) + \mu_i^r(T, \rho, x_i)$, where N_i is the number of molecules of species i , $\rho = N/V$, $x_i = N_i/N$ and ρ_{ref} is an arbitrary reference density. The expression $\mu_i - \mu_i^o(T)$ is often referred to as the configurational chemical potential μ_i^{conf} . Widom’s method requires the frequent insertion of

an additional ($i = N + 1$) test particle into the simulation volume at a random position with a random orientation. At constant temperature and constant pressure or volume the potential energy U_i of this test particle, i.e. the interaction energy with all other "real" N molecules, yields the configurational chemical potential according to

$$\mu_i^{\text{conf}} = \mu_i - \mu_i^{\circ}(T) = -k_{\text{B}}T \ln \frac{\langle V \exp(-U_i/k_{\text{B}}T) \rangle}{\langle N_i \rangle}, \quad (2)$$

where k_{B} is Boltzmann's constant. The test particle is removed immediately after the calculation of its potential energy U_i , thus it does not influence the real molecules in the system in any way. In contrast to the usual convention, the brackets $\langle \rangle$ have a dual meaning here: They stand for either NVT or NpT ensemble averages as well as an integral over all possible positions and orientations of the test particles added to the system. The density of the system has a significant influence on the accuracy of this method. For state points with a very high density, test particles almost always overlap with real molecules, which leads to a potential energy $U_i \rightarrow \infty$ and thus to a vanishing contribution to Eq. (2), resulting in poor statistics and often even to complete failure of sampling.

Thermodynamic integration is one solution to overcome the limitations of Widom's particle insertion method. The idea behind calculating the chemical potential by thermodynamic integration is to avoid insertion of test particles in a challenging system A , but rather perform it in system B for which this can be done without sampling problems. Because the chemical potential is a state property, its difference $\mu_{A,i} - \mu_{B,i}$ can be calculated along any path between states A and B , which is represented by the scalar parameter λ . It can be shown [37] that the relation between λ and $\mu_{A,i} - \mu_{B,i}$ is

$$\mu_{A,i} - \mu_{B,i} = \int_{B(\lambda_{\text{min}})}^{A(\lambda_{\text{max}})} \left\langle \frac{\partial U_i(\lambda)}{\partial \lambda} \right\rangle d\lambda. \quad (3)$$

The brackets $\langle \rangle$ in this equation denote NVT or NpT ensemble averages and U_i is the potential energy of particle i that must be a part of the system in the same way as the other molecules are. The only difference between particle i and all other molecules is that its interaction energy $U_i(\lambda)$ is scaled between states $A(\lambda_{\text{max}})$ and $B(\lambda_{\text{min}})$ with λ . As long as $\partial U_i(\lambda)/\partial \lambda$ can be calculated analytically and sampled during simulation, the actual way of scaling $U_i(\lambda)$ with λ can be chosen arbitrarily because μ_i is a state property. The integration with respect to λ is carried out numerically. Assuming that $\mu_{B,i}$ is practically zero or at least can successfully be calculated by Widom's particle insertion method for state B using Eq. (2), $\mu_{A,i}$ yields the configurational contribution to the total chemical potential. The non-linear scaling $U_i(\lambda) = \lambda^d U_i$ for $\lambda_{\text{min}} \leq \lambda \leq 1 = \lambda_{\text{max}}$ with an adaptive sampling technique [47] was implemented for MC simulations with d and λ_{min} being input parameters. This adaptive technique allows for the sampling of the entire range of $\lambda_{\text{min}} \leq \lambda \leq 1$ in a single MC run with an arbitrary resolution for numerical integration. In addition to the standard NVT and NpT ensemble MC moves, the simulation includes changes of λ controlled by a proper MC acceptance criterion, ensuring visits at each discrete λ value in the range $\lambda_{\text{min}} \leq \lambda \leq 1$. For MD simulations, changes of λ are also carried out on the fly in a single simulation, but without any acceptance criterion. A detailed description of the parameter setup is given in the supplementary material.

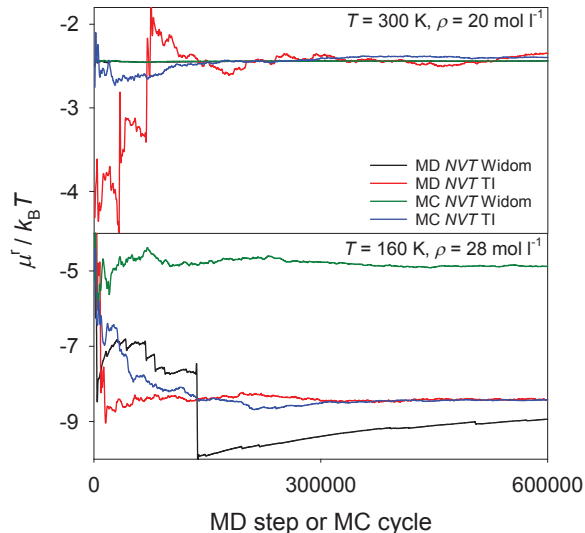


Figure 2: Comparison of the residual chemical potential μ^r of methyl fluoride [41] at two different state points calculated by *ms2* using either Widom's particle insertion or thermodynamic integration (TI).

Figure 2 shows the running averages for the residual chemical potential of methyl fluoride at two different state points calculated by either Widom's particle insertion or thermodynamic integration. For high temperatures and low densities, the agreement between Widom's particle insertion and thermodynamic integration is satisfactory. Widom fails, however, for dense and strongly interacting fluids.

5. Quaternary Maxwell-Stefan diffusion coefficients

ms2 employs the Green-Kubo formalism based on the net velocity correlation function to obtain $n \times n$ phenomenological coefficients [48]

$$L_{ij} = \frac{1}{3N} \int_0^\infty \left\langle \sum_{k=1}^{N_i} \mathbf{v}_{i,k}(0) \cdot \sum_{l=1}^{N_j} \mathbf{v}_{j,l}(t) \right\rangle dt, \quad (4)$$

in a mixture of n components. Here, N is the total number of molecules, N_i is the number of molecules of species i and $\mathbf{v}_{i,k}(t)$ denotes the center of mass velocity vector of the k -th molecule of species i at time t . Note that the phenomenological coefficients given in Eq. (4) are constrained by [48]

$$\sum_i M_i L_{ij} = 0, \quad (5)$$

where M_i is the molar mass of component i .

Starting from the phenomenological coefficients L_{ij} , the elements of a $(n-1) \times (n-1)$ matrix Δ can be defined as [48]

$$\Delta_{ij} = (1 - x_i) \left(\frac{L_{ij}}{x_j} - \frac{L_{in}}{x_n} \right) - x_i \sum_{k=1 \neq i}^n \left(\frac{L_{kj}}{x_j} - \frac{L_{kn}}{x_n} \right), \quad (6)$$

so that its inverse matrix $\mathbf{B} = \mathbf{\Delta}^{-1}$ is related to the Maxwell-Stefan diffusion coefficients \mathcal{D}_{ij} . In the case of a quaternary mixture, the six Maxwell-Stefan diffusion coefficients are then given by [48]

$$\mathcal{D}_{14} = \frac{1}{B_{11} + (x_2/x_1)B_{12} + (x_3/x_1)B_{13}}, \quad (7)$$

$$\mathcal{D}_{24} = \frac{1}{B_{22} + (x_1/x_2)B_{21} + (x_3/x_2)B_{23}}, \quad (8)$$

$$\mathcal{D}_{34} = \frac{1}{B_{33} + (x_1/x_3)B_{31} + (x_2/x_3)B_{32}}, \quad (9)$$

$$\mathcal{D}_{12} = \frac{1}{1/\mathcal{D}_{24} - B_{21}/x_2}, \quad (10)$$

$$\mathcal{D}_{13} = \frac{1}{1/\mathcal{D}_{14} - B_{13}/x_1}, \quad (11)$$

$$\mathcal{D}_{23} = \frac{1}{1/\mathcal{D}_{24} - B_{23}/x_2}. \quad (12)$$

$$(13)$$

MD simulation runs for Lennard-Jones fluids were performed in order to test the validity of the quaternary Maxwell-Stefan diffusion coefficients calculated with *ms2*. For this purpose, a quaternary Lennard-Jones pseudo-mixture was created by giving different labels to identical molecules, dividing them into four mole fractions ($x_1 = 0.1$, $x_2 = 0.2$, $x_3 = 0.3$ and $x_4 = 0.4$ mol mol⁻¹). A system containing 800 molecules was simulated in the dense liquid state and the resulting Maxwell-Stefan diffusion coefficients were compared with the corresponding self-diffusion coefficient that all have to be identical in the present case.

Fig. 3 shows the development of the calculated values of the six Maxwell-Stefan diffusion coefficients with the number of time origins. As can be seen, the resulting values become independent after around 10^4 time origins and then oscillate around their mean value. The higher statistical uncertainties of \mathcal{D}_{12} and \mathcal{D}_{13} are due to the small number of species 1 molecules compared with the number of molecules of the other species.

6. Hydrogen bonding

There is no definite characterization of a hydrogen bond between two molecules [49–51]. Rather, the hydrogen (H) bond ‘is a structural motif and involves at least three atoms’ [52]. The International Union of Pure and Applied Chemistry (IUPAC) defines the hydrogen bond as ‘an attractive interaction between a hydrogen atom from a molecule or molecular fragment X–H in which X is more electronegative than H, and an atom or a group of atoms in the same or a different molecule, in which there is evidence of bond formation’ [51].

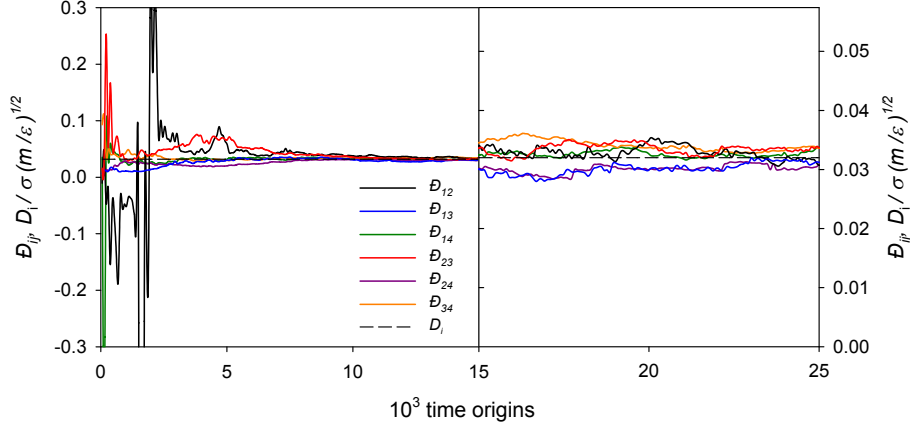


Figure 3: Maxwell-Stefan diffusion coefficients D_{ij} and the self-diffusion coefficient D_i as a function of time origins of a quaternary pseudo-mixture ($\epsilon = \epsilon_1 = \epsilon_2 = \epsilon_3 = \epsilon_4$ and $\sigma = \sigma_1 = \sigma_2 = \sigma_3 = \sigma_4$) at $k_B T / \epsilon = 0.728$ and $\rho \sigma^3 = 0.8442$.

Energetic [49], geometric [53] and topological [50] hydrogen bonding criteria have been proposed in the literature. Geometric criteria, which are not overly complex, are often based on the following assumptions [54]:

- The interaction between two hydrogen bonded sites is highly directional and short ranged.
- A donor interacts at most with a single acceptor, an acceptor may interact with multiple donors.

Accordingly, a class of geometric criteria for the evaluation of hydrogen bonding networks in fluids was implemented in *ms2*. Thereby, the triangle between three charge sites, being part of two different molecules, is evaluated to determine whether two sites constitute a hydrogen bond or not. A molecule acts as a donor to another molecule, i.e. the acceptor, if the following conditions hold [53–56], cf. Fig. 4:

- The distance between the donor and the acceptor is smaller than a threshold distance, i.e. l_{AD} or l_{DA} .
- The distance between the acceptor sites of the acceptor and donor molecules is smaller than a threshold distance, i.e. l_{AA} .
- The angle between the acceptor-donor axis and the acceptor-acceptor axis is smaller than a threshold angle, i.e. φ_{DAA} or φ_{AAD} .

Therein, l_{AD} , l_{DA} , l_{AA} , φ_{DAA} and φ_{AAD} are parameters of the implemented class of hydrogen bonding criteria. For methanol, e.g., Haughney et al. [53] proposed $l_{AD} = l_{DA} = 2.6 \text{ \AA}$, $l_{AA} = 3.5 \text{ \AA}$ and $\varphi_{AAD} = \varphi_{DAA} = 30^\circ$. Such geometric criteria have been applied to a variety of fluids, in

particular to water [55–57], methanol-water mixtures [58, 59] or ethanol [54, 60, 61]. Hydrogen bonds in sorbate-sorbent interactions can be treated analogously [62]. E.g., for hydrogen fluoride, a simpler distance-based criterion can be used [63], which is also covered by the present implementation. A detailed description of the parameter setup is given in the supplementary material.

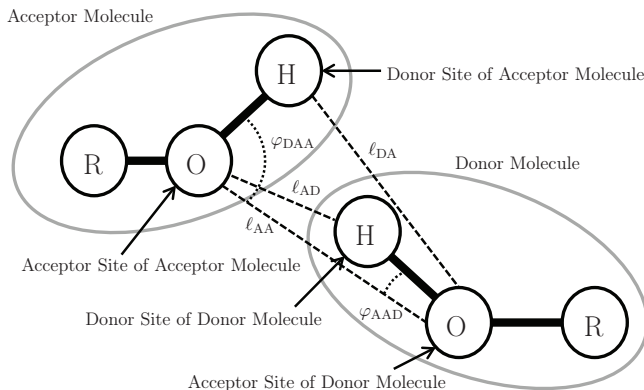


Figure 4: Hydrogen bonding criteria implemented in the present release version of *ms2*.

To test the capabilities of the hydrogen bonding statistics implemented in *ms2*, a MD simulation run of the ternary mixture water (w) + methanol (m) + ethanol (e) ($x_w = 0.33$, $x_m = 0.33$, $x_e = 0.34$ mol mol⁻¹) at $T = 298.15$ K and $p = 0.1$ MPa was carried out with 4000 molecules. In this mixture all species can form hydrogen bonds with each other because all three molecules contain hydroxyl groups. Thus the hydrogen atoms may act as donors and the oxygen atoms as acceptors to form hydrogen bonds. Throughout, between like and unlike molecules, the geometric criteria of Haughney et al. [53] were used. The results are listed in Table 3. The hydrogen bonding statistics in *ms2* not only indicates the amount of monomers (no bond), dimers (one bond), trimers (two bonds) and tetramers (three bonds), but also provides information about which molecule species are bonded.

7. OPAS Method

The OPAS (osmotic pressure for the activity of the solvent) method was implemented in *ms2*. It is an alternative to e.g. the Widom’s particle insertion [46] or thermodynamic integration [64–66], for calculating chemical potentials in the liquid phase by MD simulations. It is particularly well-suited for studying the solvent activity of electrolyte solutions, but can in principle also be used for mixtures of molecular species. Details and a thorough assessment of the method are presented in Ref. [67], the method is only briefly outlined in the following.

The basic idea is a direct simulation of the osmotic equilibrium between a pure solvent phase and a solution phase by introducing semi-permeable membranes into the simulation volume. These are realized by an external force field that acts only on the solute molecules to keep them in the solution phase. By sampling the total net membrane force per membrane area, the pressure difference between the two phases, i.e. the osmotic pressure Π , is sampled. Assuming an incompressible

Table 3: Hydrogen bonding statistics of the ternary mixture water (w) + methanol (m) + ethanol (e) ($x_w = 0.33$, $x_m = 0.33$, $x_e = 0.34$ mol mol⁻¹) at $T = 298.15$ K and $p = 0.1$ MPa in relative terms.

	water	methanol	ethanol
monomer	0.1%	0.9%	1.1%
dimer	1.2%	10.6%	11.5%
bonded to (w)	0.8%	3.5%	4.1%
(m)	0.2%	3.3%	3.6%
(e)	0.2%	3.8%	3.8%
trimer	7.8%	47.7%	42.6%
bonded to (w)(w)	2.8%	2.8%	2.8%
(w)(m)	1.9%	10.5%	8.9%
(w)(e)	2.0%	12.3%	10.2%
(m)(m)	0.3%	5.0%	4.9%
(m)(e)	0.4%	11.0%	10.3%
(e)(e)	0.4%	6.1%	5.5%
tetramer	25.8%	35.9%	36.8%
bonded to (w)(w)(w)	3.9%	15.6%	12.7%
(w)(w)(m)	4.9%	7.6%	7.8%
(w)(w)(e)	5.1%	7.7%	7.6%
(w)(m)(m)	2.7%	0.7%	1.3%
(w)(m)(e)	3.8%	1.7%	2.8%
(w)(e)(e)	2.8%	0.9%	1.5%
(m)(m)(m)	0.6%	0.2%	0.4%
(m)(m)(e)	0.7%	0.6%	1.1%
(m)(e)(e)	0.6%	0.7%	1.2%
(e)(e)(e)	0.7%	0.2%	0.4%
four or more bonds	65.1%	4.9%	8.0%

solvent, the solvent activity is related to this osmotic pressure by

$$\ln a_s = -\frac{\Pi v_s}{RT}, \quad (14)$$

where v_s is the molar volume of the pure solvent at the temperature T , which is straightforwardly available from separate, standard molecular simulation runs. If an electrolyte solution is considered, the activity coefficient of the salt can be obtained by performing OPAS simulations at various salt molalities and applying the Gibbs-Duhem equation to the results for the solvent activity.

Fig. 5 shows molecular simulation results for the mean ionic activity coefficient of NaCl in aqueous solution at $T = 298.15$ K and $p = 1$ bar. Therein, results obtained by different groups, employing different computational approaches, are presented. Throughout, the molecular models by Joung and Cheatham [68] for Na^+ and Cl^- ions together with the SPC/E water model were used, and all simulation results are in mutual agreement.

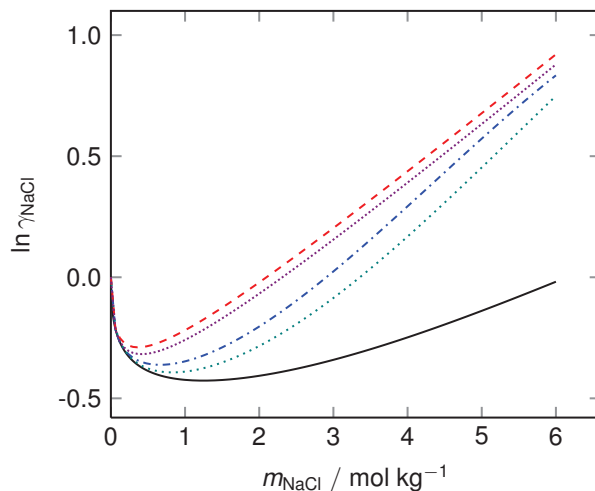


Figure 5: Mean ionic activity coefficient of NaCl over salt molality for aqueous NaCl solutions at $T = 298.15$ K and $p = 1$ bar using the SPC/E + Joung-Cheatham [68] model combination. The colored lines represent simulation results by different groups for that model combination (from top to bottom): OPAS simulations by Kohns et al. [67] (red dashed line), free energy calculations by Benavides et al. [69] (violet densely-dotted line), gradual insertion of ion pairs by Mester and Panagiotopoulos [65] (blue dashed-dotted line), and osmotic ensemble Monte Carlo simulations by Moučka et al. [66] (green dotted line). The black solid line shows the correlation to experimental data by Hamer and Wu [70].

8. Electrostatic long range corrections

The applicability of *ms2* was extended to electrically charged molecules or ions. The long ranged intermolecular interactions are considered by two well established approaches, Ewald summation and smooth-particle mesh Ewald summation (SPME). Both are well known [37] and are thus introduced here only briefly.

In Ewald summation, the overall Coulombic potential acting in the simulation volume is determined by a sum of two terms, i.e. the short range Coulombic contribution $u^{c,\text{short}}$ and the long range Coulombic contribution $u^{c,\text{long}}$

$$u^c = u^{c,\text{short}} + u^{c,\text{long}} . \quad (15)$$

The separation into these terms is achieved by the introduction of a fictive charge density function $\rho^{\text{screen}}(\mathbf{r})$, which acts in the entire simulation volume.

Following the Ewald summation approach, for any configuration of molecules in the simulation volume, each point charge of magnitude q_l in the simulation volume is superimposed with one countercharge of magnitude $-q_l$. Due to the presence of this superimposed charge, the interaction potential decays to zero within a distance that is reasonably short for molecular simulation and can, hence, be explicitly considered by the short term contribution of the Ewald summation.

The second term in Eq. (15) determines the contribution that was subtracted due to the introduction of the fictive charge density function. This term cannot be determined explicitly by the evaluation of pairwise interactions, since the Coulombic potential at $r_{lm} = V^{1/3}/2$, i.e. the largest distance accessible in the molecular simulation volume V , is still a substantial part of the potential energy of the system. In Ewald summation, this contribution is determined in Fourier space from the negative charge distribution function $-\rho^{\text{screen}}(\mathbf{r})$. Since $\rho^{\text{screen}}(\mathbf{r})$ depends on the molecular positions \mathbf{r} , a Fourier transformation is performed for every configurational change in the simulation volume.

The SPME is widely considered as an improved Ewald summation method. In this approach, the concept of splitting the long range charge-charge interactions is fully employed. The difference between both methods lies only in the calculation of the long range contributions. In the SPME approach, the electrostatic field of ions in the simulation volume is described by a spline function with a given functional form. For this given spline equation, the Fourier transformation is known and has, hence, not to be determined in each simulation step. This accelerates the calculation of the long range contribution and reduces simulation effort and time. The accuracy of the SPME results is assumed to be equivalent to the Ewald approach. In *ms2* release 3.0, the SPME method was implemented in its original form wherein the splines are evaluated for all particles at a time, making it specifically useful for MD simulations. Typical systems show an improved performance of up to 21% in total computational time.

9. Vectorization

For the vectorization of loops it is essential how accessed data are distributed in physical memory. Deducing this information automatically from the code can be very difficult for the compiler, especially if there is indirection. In *ms2*, many arrays are accessed via array pointers and the order of the underlying data is therefore obfuscated. The most relevant information is whether or not data are contiguous in physical memory. To provide this information to the compiler directly, array pointers can be given the attribute "contiguous". The Fortran standard specifies: "*The contiguous attribute specifies that [...] an array pointer can only be pointer associated with a contiguous target.*" This means that the array elements of a contiguous array pointer are not

separated by any other data, potentially enabling a higher degree of vectorization. In *ms2* release 3.0, array pointers associated with contiguous targets have been given the contiguous attribute. The sequential performance gains and the resulting parallel performance gains achieved with this optimization depend on the specific simulation scenario, but are on average very significant. For MC and MD simulations, a suite of simulations was executed to evaluate the performance gains. The suite covered the NpT and NVT ensembles, thermodynamic integration, Widom test particle insertion, different thermostats, different pure fluids and mixtures. A total of 71 simulation runs was performed. For MC simulations, the observed average reduction of runtime was more than 7% and for MD simulations more than 20%.

10. Parallel ensemble calculations

ms2 was already parallelized in its initial version for distributed memory architectures using the message passing interface (MPI) [9, 10]. The present release 3.0 adds an additional level of parallelization for MD simulations. Different ensembles are independent of each other in the sense that sampling different state points can be done concurrently. To achieve this, the processing elements (PE) are split in disjunct groups and each group computes the ensembles assigned to it. To enable this feature, the *mpiEnsembleGroups* option was introduced in the input file. The default (if not set or set to 0) is to use a single ensemble group. A value of 1 will enable the new feature and automatically set the number of ensemble groups to the minimum of the number of ensembles and the number of PE, i.e. $mpiEnsembleGroups = \min(\text{ensembles}, \text{PE})$. Otherwise, this option will set the number of ensemble groups according to the specified integer value. The “coloring”, i.e. the assignment of the PE to the ensemble groups, is done in contiguous blocks. This is advantageous, e.g. compared to a round robin fashion, if the processes have to be pinned to NUMA domains.

Another change applies to the restart capability of *ms2*. A checkpoint now consists of one restart (*.rst) file for each ensemble group that can be restarted with the *ms2* -r (or --restart) option.

To illustrate the new feature, a MD program execution for three ensembles with 24 processes will serve as an example. Without the *mpiEnsembleGroups* option (or with $mpiEnsembleGroups=0$) all 24 PE will in parallel calculate the first time step of the first ensemble, then the first time step of the second ensemble and finally the first time step of the third one, before the second time step is handled accordingly. Setting $mpiEnsembleGroups=1$ is equivalent to $mpiEnsembleGroups=3$ in this example and three groups of eight PE each will calculate one ensemble in parallel concurrently. The user may also directly specify the number of groups, but has to be aware that in this example with $mpiEnsembleGroups=2$ one group will have to process two ensembles, while the other one only processes a single one.

ms2 creates a MPI communicator for each of the ensemble groups with the MPI_Comm.Split command, cf. Figure 6. Another MPI communicator contains the root processes of all groups (Communicator_R including subcommunicators rank 0 processes) to ease collective communication on a higher level among the groups.

Even if the computation of different ensembles is embarrassingly parallel, an interaction between the different ensemble groups through communicators remains, e.g. when the program receives a signal to write a checkpoint and terminate. This signal may be received from an arbitrary single PE

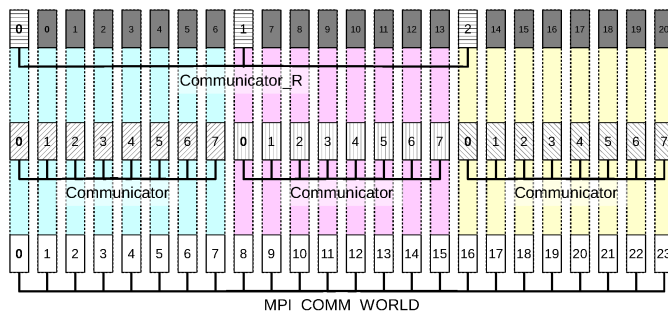


Figure 6: MPI ranks for 24 PE in 3 MPI groups, indicating communicator hierarchy of *ms2*.

(or non-isochronic from multiple PE). In the preceding releases of *ms2*, where ensembles were calculated consecutively with the single global communicator `MPI_COMM_WORLD`, a `MPI_Allreduce` spreads this information among all processes after every MD time step. This is still the case within the ensemble groups. A collective communication of all PE beyond ensemble group boundaries for every MD time step would implicitly synchronize all ensemble computations. However, this is not satisfactory because computationally less intensive ensembles would be forced to wait for slower ones to conclude their time step. The present implementation uses non-blocking communication between the ensemble group roots through `Communicator_R` to avoid this problem.

Before any MD time step iterations start, the root process executes a `MPI_Irecv` call to receive a potential terminate message, whereas all other processes execute a `MPI_Ibcast` to obtain a potential terminate message from the root, cf. Figure 7. During program execution, any process may trigger termination by sending a message to the root, which will then broadcast the information to notify all other processes. If no termination occurs during the iterations, the root will send a message to itself and broadcast a non-termination message to all other processes to satisfy the outstanding receive and broadcast (avoiding `MPI_Cancel`). To take care of several processes sending a termination message, a summation reduction determines the sum of all respective messages for the root process to receive all of them. This technique can also be used hierarchically, replacing the `MPI_Allreduce` call within each subcommunicator. After termination, every ensemble group writes its own restart (*.rst) file.

Acknowledgements

The authors gratefully acknowledge financial support by BMBF under the grant “01IH13005A SkaSim: Skalierbare HPC-Software für molekulare Simulationen in der chemischen Industrie” and computational support by the High Performance Computing Center Stuttgart (HLRS) under the grant MMHBF2. Furthermore, we gratefully acknowledge the Paderborn Center for Parallel Computing (PC²) for the generous allocation of computer time on the OCuLUS cluster. The present research was conducted under the auspices of the Boltzmann-Zuse Society of Computational Molecular Engineering (BZS). H.H. and M.K. acknowledge support of this work by DFG under a Reinhart Koselleck grant.

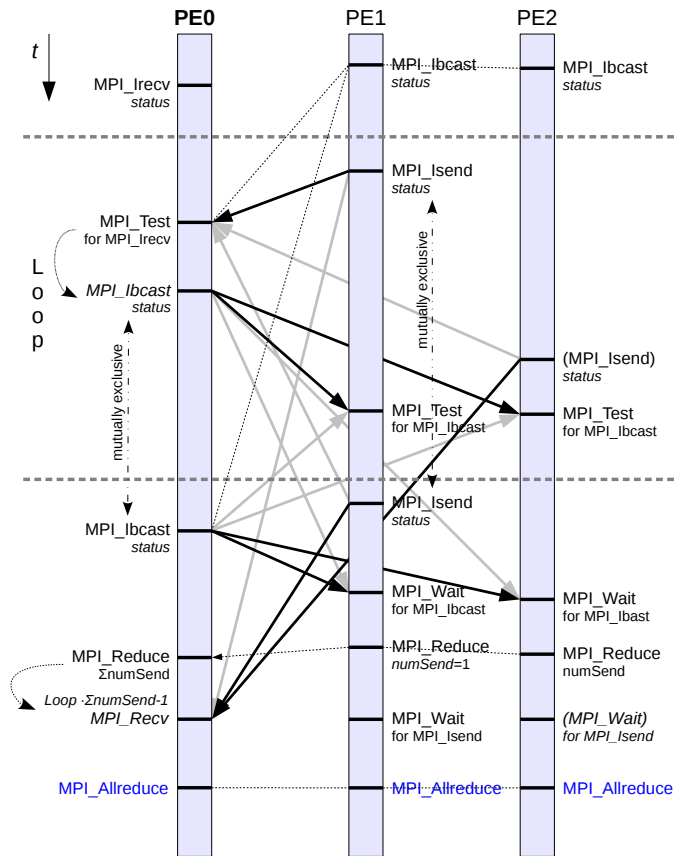


Figure 7: Communication to distribute status information within a MD time step avoiding barriers. Thick solid arrows indicate communication among PE (grey arrows for alternative possible receiving points). Dotted lines between the PE indicate collective communication implicating a barrier. For mutually exclusive commands, the second one is only executed if the first one was not triggered.

- [1] P. Ungerer, C. Nieto-Draghi, B. Rousseau, G. Ahunbay, V. Lachet, *J. Mol. Liq.* 134 (2007) 71–89.
- [2] J. C. Palmer, P. G. Debenedetti, *AIChE J.* 61 (2015) 370–383.
- [3] A. Heinecke, W. Eckhardt, M. Horsch, H.-J. Bungartz, *Supercomputing for Molecular Dynamics Simulations*, Springer Verlag, Heidelberg, 2015.
- [4] A. Köster, T. Jiang, G. Rutkai, C. W. Glass, J. Vrabec, *Fluid Phase Equilib.* 425 (2016) 84–92.
- [5] C. Valeriani, R. J. Allen, M. J. Morelli, D. Frenkel, P. R. ten Wolde, *J. Chem. Phys.* 127 (2007) 114109.
- [6] D. R. Glowacki, E. Paci, D. V. Shalashilin, *J. Chem. Theory Comput.* 7 (2011) 1244–1252.
- [7] S. L. Meadley, F. A. Escobedo, *J. Chem. Phys.* 137 (2012) 074109.

- [8] URL <http://www.ms-2.de/>.
- [9] S. Deublein, B. Eckl, J. Stoll, S. V. Lishchuk, G. Guevara-Carrion, C. W. Glass, T. Merker, M. Bernreuther, H. Hasse, J. Vrabec, *Comput. Phys. Commun.* 182 (2011) 2350–2367.
- [10] C. W. Glass, S. Reiser, G. Rutkai, S. Deublein, A. Köster, G. Guevara-Carrion, A. Wafai, M. Horsch, M. Bernreuther, T. Windmann, H. Hasse, J. Vrabec, *Comput. Phys. Commun.* 185 (2014) 3302–3306.
- [11] C. Nieto-Draghi, P. Bonnaud, P. Ungerer, *J. Phys. Chem. C* 111 (2007) 15942–15951.
- [12] E. El Ahmar, B. Creton, A. Valtz, C. Coquelet, V. Lachet, D. Richon, P. Ungerer, *Fluid Phase Equilib.* 304 (2011) 21–34.
- [13] Y.-L. Huang, M. Heilig, H. Hasse, J. Vrabec, *AIChE J.* 57 (2011) 1043–1060.
- [14] M. H. Ketko, G. Kamath, J. J. Potoff, *J. Phys. Chem. B* 115 (2011) 4949–4954.
- [15] S. Reiser, M. Horsch, H. Hasse, *J. Chem. Eng. Data* 60 (2015) 1614–1628.
- [16] S. Werth, K. Stöbener, P. Klein, K.-H. Küfer, M. Horsch, H. Hasse, *Chem. Eng. Sci.* 121 (2015) 110–117.
- [17] R. Srivastava, H. Docherty, J. K. Singh, P. T. Cummings, *J. Phys. Chem. C* 115 (2011) 12448–12457.
- [18] L. Lu, S. Wang, E. A. Müller, W. Cao, Y. Zhu, X. Lu, G. Jackson, *Fluid Phase Equilib.* 362 (2014) 227–234.
- [19] A. Sharma, S. Namsani, J. K. Singh, *Mol. Sim.* 41 (2015) 414–422.
- [20] J. L. Kern, T. J. Flynn, Z. Wang, W. H. Thompson, B. B. Laird, *Fluid Phase Equilib.* 411 (2016) 81–87.
- [21] J. Muscatello, F. Jaeger, O. K. Matar, E. A. Müller, *Appl. Mater. Interf.* 8 (2016) 12330–12336.
- [22] B. R. Brooks, C. L. Brooks, A. D. Mackerell, L. Nilsson, R. J. Petrella, B. Roux, Y. Won, G. Archontis, C. Bartels, S. Boresch, A. Caffisch, L. Caves, Q. Cui, A. R. Dinner, M. Feig, S. Fischer, J. Gao, M. Hodoscek, W. Im, K. Kuczera, T. Lazaridis, J. Ma, V. Ovchinnikov, E. Paci, R. W. Pastor, C. B. Post, J. Z. Pu, M. Schaefer, B. Tidor, R. M. Venable, H. L. Woodcock, X. Wu, W. Yang, D. M. York, M. Karplus, *J. Comp. Chem.* 30 (2009) 1545–1614.
- [23] I. T. Todorov, W. Smith, K. Trachenko, M. T. Dove, *J. Mater. Chem.* 16 (2006) 1911–1918.
- [24] H.-J. Limbach, A. Arnold, B. A. Mann, C. Holm, *Comp. Phys. Comm.* 174 (2006) 704–727.
- [25] M. Lagache, P. Ungerer, A. Boutin, A. Fuchs, *Phys. Chem. Chem. Phys.* 3 (2001) 4333–4339.

- [26] M. J. Abraham, T. Murtola, R. Schulz, S. Páll, J. C. Smith, B. Hess, E. Lindahl, *SoftwareX* 1 (2015) 19–25.
- [27] J. Roth, F. Gähler, H.-R. Trebin, *Int. J. Mod. Phys. C* 11 (2000) 317–322.
- [28] S. Plimpton, *J. Comp. Phys.* 117 (1995) 1–19.
- [29] C. Niethammer, S. Becker, M. Bernreuther, M. Buchholz, W. Eckhardt, A. Heinecke, S. Werth, H.-J. Bungartz, C. W. Glass, H. Hasse, J. Vrabec, M. Horsch, *J. Chem. Theory Comput.* 10 (2014) 4455–4464.
- [30] J. C. Phillips, R. Braun, W. Wang, J. Gumbart, E. Tajkhorshid, E. Villa, C. Chipot, R. D. Skeel, L. Kale, K. Schulten, *J. Comp. Chem.* 26 (2005) 1781–1802.
- [31] P. Ren, J. W. Ponder, *J. Phys. Chem. B* 107 (2003) 5933–5947.
- [32] M. G. Martin, *Mol. Sim.* 39 (2013) 1212–1222.
- [33] M. Thol, G. Rutkai, A. Köster, R. Lustig, R. Span, J. Vrabec, *J. Phys. Chem. Ref. Data* 45 (2016) 023101.
- [34] M. Hülsmann, T. Köddermann, J. Vrabec, D. Reith, *Comput. Phys. Commun.* 181 (2010) 499–513.
- [35] M. Hülsmann, J. Vrabec, A. Maaß, D. Reith, *Comput. Phys. Commun.* 181 (2010) 887–905.
- [36] K. Stöbener, P. Klein, S. Reiser, M. Horsch, K.-H. Küfer, H. Hasse, *Fluid Phase Equilib.* 373 (2014) 100–108.
- [37] D. Frenkel, B. Smit, *Understanding Molecular Simulation: From Algorithms to Applications*, Academic Press, Elsevier, San Diego, 2002.
- [38] R. Lustig, *J. Chem. Phys.* 109 (1998) 8816–8828.
- [39] T. Kristóf, G. Rutkai, L. Merényi, J. Liszi, *Mol. Phys.* 103 (2005) 537–545.
- [40] H. C. Andersen, *J. Chem. Phys.* 72 (1980) 2384–2393.
- [41] J. Vrabec, J. Stoll, H. Hasse, *J. Phys. Chem. B* 105 (2001) 12126–12133.
- [42] H. Flyvbjerg, H. G. Petersen, *J. Chem. Phys.* 91 (1989) 461–466.
- [43] R. Span, *Multiparameter Equations of State: An Accurate Source of Thermodynamic Property Data*, Springer Verlag, Berlin, 2000.
- [44] R. Lustig, *Mol. Sim.* 37 (2011) 457–465.
- [45] R. Lustig, *Mol. Phys.* 110 (2012) 3041–3052.

- [46] B. Widom, *J. Chem. Phys.* 39 (1963) 2808–2812.
- [47] T. Kristóf, G. Rutkai, *Chem. Phys. Lett.* 445 (2007) 74–78.
- [48] R. Krishna, J. M. van Baten, *Ind. Eng. Chem. Res.* 44 (2005) 6939–6947.
- [49] F. H. Stillinger, *Science* 209 (1980) 451–457.
- [50] R. H. Henchman, S. J. Irudayam, *J. Phys. Chem. B* 114 (2010) 16792–16810.
- [51] E. Arunan, G. R. Desiraju, R. A. Klein, J. Sadlej, S. Scheiner, I. Alkorta, D. C. Clary, R. H. Crabtree, J. J. Dannenberg, P. Hobza, H. G. Kjaergaard, A. C. Legon, B. Mennucci, D. J. Nesbitt, *Pure Appl. Chem.* 83 (2011) 1637–1641.
- [52] J. Thar, B. Kirchner, *J. Phys. Chem. A* 110 (2006) 4229–4237.
- [53] M. Haughney, M. Ferrario, I. R. McDonald, *J. Phys. Chem.* 91 (1987) 4934–4940.
- [54] S. Reiser, N. McCann, M. Horsch, H. Hasse, *J. Supercrit. Fluids* 68 (2012) 94–103.
- [55] A. Luzar, D. Chandler, *J. Chem. Phys.* 98 (1993) 8160–8173.
- [56] S. Chowdhuri, A. Chandra, *J. Phys. Chem. B* 110 (2006) 9674–9680.
- [57] A. Luzar, D. Chandler, *Nature* 379 (1996) 55–57.
- [58] J. R. Choudhuri, A. Chandra, *J. Chem. Phys.* 141 (2014) 134703.
- [59] G. Guevara-Carrion, C. Nieto-Draghi, J. Vrabc, H. Hasse, *J. Phys. Chem. B* 112 (2008) 16664–16674.
- [60] L. Saiz, J. A. Padró, E. Guàrdia, *J. Phys. Chem. B* 101 (1997) 78–86.
- [61] W. Xu, J. Yang, Y. Hu, *J. Phys. Chem. B* 113 (2009) 4781–4789.
- [62] D. Bhandary, S. Khan, J. K. Singh, *J. Phys. Chem. C* 118 (2014) 6809–6819.
- [63] M. Kreitmeir, H. Bertagnolli, J. J. Mortensen, M. Parrinello, *J. Chem. Phys.* 118 (2003) 3639–3645.
- [64] F. Moučka, I. Nezbeda, W. R. Smith, *J. Chem. Phys.* 139 (2013) 124505.
- [65] Z. Mester, A. Z. Panagiotopoulos, *J. Chem. Phys.* 142 (2015) 044507.
- [66] F. Moučka, I. Nezbeda, W. R. Smith, *J. Chem. Theory Comput.* 11 (2015) 1756–1764.
- [67] M. Kohns, S. Reiser, M. Horsch, H. Hasse, *J. Chem. Phys.* 144 (2016) 084112.
- [68] I. S. Joung, T. E. Cheatham, *J. Phys. Chem. B* 112 (2008) 9020–9041.

[69] A. L. Benavides, J. L. Aragoes, C. Vega, *J. Chem. Phys.* 144 (2016) 124504.

[70] W. J. Hamer, Y. Wu, *J. Phys. Chem. Ref. Data* 1 (1972) 1047–1100.

SUPPLEMENTARY INFORMATION: Hydrogen bonding

The user has to specify the geometric relations in the `*.par` file according to the simulated components as follows: First, the keyword `NHBondCriteria = '#h-bonds'` has to be set to the integer value `#h-bonds` according to the number of different H bonds that shall be investigated during the simulation. This keyword has to appear under the components section in the `*.par` file. `#h-bonds` also sets the number of lines that `ms2` expects in the `*.par` file, each to have a complete set of nine parameters that declare a certain H bond. These nine parameters are:

`AccComp`, `AccAccSite`, `AccDonSite`, `DonComp`, `DonAccSite`, `DonDonSite`, `DistCrit1`, `DistCrit2` and `AngleCrit`. The first six parameters declare which charge – charge interactions of which component are to be considered by `ms2`. The acceptor and donor sites listed in the `*.par` file have to be point charges listed in the `*.pm` file. `AccComp` and `DonComp` are the component numbers of the components that are supposed to be the acceptor and donor of the H bond, respectively. Both have to be integer values according to the order of the components listed in the `*.par` file. The four charge sites that participate in the H bond have to be set by the user as `AccAccSite`, `AccDonSite`, `DonAccSite` and `DonDonSite`. They have to be integer values according to the order of the charge sites listed in the `*.pm` file. `AccAccSite` and `AccDonSite` are the acceptor and donor charge sites in the component that is acting as the acceptor molecule in the H bond while `DonAccSite` and `DonDonSite` are the acceptor and donor charge-sites in the donor molecule. As mentioned, only three charge sites are needed for the criterion, thus either the `AccDonSite` or the `DonDonSite` has to be set to 0 by the user as can be seen in table 1. This is equivalent of defining either ℓ_{DA} and φ_{DAA} or ℓ_{AD} and φ_{AAD} .

The last three numeric parameters in table 1 are the actual geometric length ℓ_{AA} , ℓ_{AD} or ℓ_{DA} and angles φ_{DAA} or φ_{AAD} as described in [Haughney et al., J, Chem. Phys., 91(1987) 4934–4940]. `ms2` always expects these values to be specified in Ångstrom and degree, respectively, independent of the settings of the `Units` keyword in the `*.par` file before.

DistCrit1: $|\ell_{AA}| = 1^{\text{st}}$ Distance criterion in Å

DistCrit2: $|\ell_{DA}|$ or $|\ell_{AD}| = 2^{\text{nd}}$ Distance criterion in Å

AngleCrit: φ_{DAA} or $\varphi_{AAD} =$ Angle criterion in $^{\circ}$

Table 1 gives two examples for a complete parameter set to be specified in a `*.par` file. During

Table 1: Example of Parameter sets for H bonding criterion.

AccComp	AccAccSite	AccDonSite	DonComp	DonAccSite	DonDonSite	DistCrit1	DistCrit2	AngleCrit
1	2	0	1	2	3	3.5	2.6	30
1	2	3	1	2	0	3.5	2.6	30

simulation, `ms2` lists the analysis of the H bonding in the `*.rav` file. Following the *Haughney*-criterion, `ms2` calculates and itemizes the number N_i of molecules with $i = 0, 1, 2, 3$ or more hydrogen bonds. In the `*.rav` file these numbers are listed according to the component combination. E.g. the `N3_(1, 2, 2, 3)` column lists the number of molecules which correspond to component 1 and are bonded twice with component 2 and once with component 3. As usual for the `*.rav` file, these values are running averages.

$$|\underline{\ell}_{AA}| \geq |r_{\text{AccAccSite}} - r_{\text{DonAccSite}}| \quad (1)$$

$$|\underline{\ell}_{DA}| \geq |r_{\text{AccDonSite}} - r_{\text{DonAccSite}}| \quad (2)$$

$$|\underline{\ell}_{AD}| \geq |r_{\text{AccAccSite}} - r_{\text{DonDonSite}}| \quad (3)$$

$$\varphi_{\text{DAA}} \leq \arccos \left| \frac{(r_{\text{AccDonSite}} - r_{\text{AccAccSite}}) \cdot \underline{\ell}_{AA}}{|r_{\text{AccDonSite}} - r_{\text{AccAccSite}}| \cdot |\underline{\ell}_{AA}|} \right| \quad (4)$$

$$\varphi_{\text{AAD}} \leq \arccos \left| \frac{(r_{\text{DonAccSite}} - r_{\text{DonDonSite}}) \cdot \underline{\ell}_{AA}}{|r_{\text{DonAccSite}} - r_{\text{DonDonSite}}| \cdot |\underline{\ell}_{AA}|} \right| \quad (5)$$

SUPPLEMENTARY INFORMATION: Thermodynamic Integration

There are four parameters (`LambdaMin`, `NBins`, `LambdaStepMax` and `LambdaExponent`) involved with the present approach that the user has to specify after the entry `ChemPotMethod = ThermoInt` in the `*.par`.

- **LambdaMin:** The lower boundary of the interval $\lambda_{\min} \leq \lambda \leq 1$ (default value is 0.2 if not specified).
- **NBins:** The number of discrete λ -bins in the interval $\lambda_{\min} \leq \lambda \leq 1$ used for the numerical integration (default value is 100 if not specified). The resolution is $(1 - \text{LambdaMin})/\text{NBins}$. During the simulation the current bin is determined by $(\lambda - \text{LambdaMin})/\text{NBins}$ for the current λ .
- **LambdaStepMax:** Defines the change of λ during simulation. The new λ is the current λ plus a random number between zero and $\pm \text{LambdaStepMax}$ (default value is 0.1 if not specified).
- **LambdaExponent:** The exponent d for the non-linear scaling $U_j(\lambda) = \lambda^d U_j$ ($\lambda_{\min} \leq \lambda \leq 1$) (it does not have to be an integer and its default value is 4.0 if not specified).

One should keep in mind when choosing these parameters that thermodynamic integration always involves larger statistical uncertainties than the equivalent pure Widom's particle insertion scenario for a state point for which the latter works perfectly. In other words: The larger the contribution of the numerical integration part as compared to the Widom contribution at λ_{\min} is, the higher the statistical uncertainty of the calculated chemical potential gets. This means that setting λ_{\min} very low or the exponent d very high (e.g. 12) might not be optimal in many systems. Moreover, high exponent d values for MD simulations are not advised because the scaling with d at high λ values (where the absolute value of $U_j(\lambda)$ is close that of the non-scaled state) may result in new $U_j(\lambda)$ energies (thus forces) that non-negligibly interfere with the dynamics of the system when λ is changed during the simulation. For MD simulations, a value smaller than 1.0 for d is possibly a better choice for many systems.

1 Potential Models in the ms2-distribution

Filename	CAS number	Name	Publication	Model Type
Ar.pm	7440-37-1	Argon	[Vrabec et al. 2001]	1 L.J. Center
Ba2+.pm	22541-12-4	Barium ion (2+)	[Deublein et al. 2012]	1 L.J. Center & 1 Charge
Be2+.pm	22537-20-8	Beryllium ion (2+)	[Deublein et al. 2012]	1 L.J. Center & 1 Charge
Br-_I.pm	24959-67-9	Bromine ion (1-)	[Deublein et al. 2012]	1 L.J. Center & 1 Charge
Br-_II.pm	24959-67-9	Bromine ion (1-)	[Deublein et al. 2012]	1 L.J. Center & 1 Charge
Br2.pm	7726-95-6	Bromine	[Vrabec et al. 2001]	2 L.J. Centers & 1 Quadrupole
C2Br2F4.pm	124-73-2	1,2-Dibromotetrafluoroethane	[Stoll et al. 2003]	2 L.J. Centers & 1 Quadrupole
C2Cl4.pm	127-18-4	Tetrachloroethylene	[Stoll 2004]	2 L.J. Centers & 1 Quadrupole
C2ClF3.pm	79-38-9	Chlorotrifluoroethene	[Stoll et al. 2003]	2 L.J. Centers & 1 Dipole
C2F4.pm	116-14-3	Tetrafluoroethylene	[Stoll 2004]	2 L.J. Centers & 1 Quadrupole
C2F6.pm	76-16-4	Perfluoroethane	[Stoll 2004]	2 L.J. Centers & 1 Quadrupole
C2H2.pm	74-86-2	Acetylene	[Vrabec et al. 2001]	2 L.J. Centers & 1 Quadrupole
C2H2Cl3F.pm	27154-33-2	Ethane, trichlorofluoro-	[Stoll et al. 2003]	2 L.J. Centers & 1 Dipole
C2H2Cl4_I.pm	630-20-6	1,1,1,2-Tetrachloroethane	[Stoll 2004]	2 L.J. Centers & 1 Dipole
C2H2Cl4_II.pm	630-20-6	1,1,1,2-Tetrachloroethane	[Stoll et al. 2003]	2 L.J. Centers & 1 Dipole
C2H2F2.pm	75-38-7	1,1-Difluoroethene	[Stoll et al. 2003]	2 L.J. Centers & 1 Dipole
C2H3Cl.pm	75-01-4	Vinyl chloride	[Stoll et al. 2003]	2 L.J. Centers & 1 Dipole
C2H3Cl3_a.pm	71-55-6	Methylchloroform	[Stoll et al. 2003]	2 L.J. Centers & 1 Dipole
C2H3Cl3_b.pm	79-00-5	1,1,2-Trichloroethane	[Stoll et al. 2003]	2 L.J. Centers & 1 Dipole
C2H3F.pm	75-02-5	Vinyl fluoride	[Stoll et al. 2003]	2 L.J. Centers & 1 Dipole
C2H3N.pm	75-05-8	Acetonitrile	[Eckl et al. 2008c]	3 L.J. Centers & 1 Dipole & 1 Quadrupole
C2H3N_m6.pm	75-05-8	Acetonitrile	[Deublein et al. 2013]	3 L.J. Centers & 1 Dipole
C2H3N_m8.pm	75-05-8	Acetonitrile	[Deublein et al. 2013]	3 L.J. Centers & 1 Dipole
C2H4.pm	74-85-1	Ethylene	[Vrabec et al. 2001]	2 L.J. Centers & 1 Quadrupole
C2H4Br2.pm	106-93-4	Ethylene dibromide	[Stoll et al. 2003]	2 L.J. Centers & 1 Quadrupole
C2H4Br3.pm	557-91-5	1,1-Dibromoethane	[Stoll et al. 2003]	2 L.J. Centers & 1 Dipole
C2H4Cl2.pm	75-34-3	1,1-Dichloroethane	[Stoll et al. 2003]	2 L.J. Centers & 1 Dipole
C2H4O_I.pm	75-21-8	Ethylene oxide	[Eckl et al. 2008b]	3 L.J. Centers & 1 Dipole
C2H5Br.pm	74-96-4	Ethyl bromide	[Stoll et al. 2003]	2 L.J. Centers & 1 Dipole
C2H5F.pm	353-36-6	Fluoroethane	[Stoll et al. 2003]	2 L.J. Centers & 1 Dipole
C2H6_I.pm	74-84-0	Ethane	[Vrabec et al. 2001]	2 L.J. Centers & 1 Quadrupole
C2H6_II.pm	74-84-0	Ethane	[Stoll 2004]	2 L.J. Centers & 1 Quadrupole
C2H6O.pm	64-17-5	Ethanol	[Schnabel et al. 2005]	3 L.J. Centers & 3 Charges
C2H6O2.pm	107-21-1	Ethylene glycol	[Huang et al. 2012]	4 L.J. Centers & 6 Charges
C2H6S_I.pm	75-18-3	Dimethyl sulfide	[Eckl et al. 2008c]	3 L.J. Centers & 1 Dipole & 2 Quadrupoles
C2H8N2.pm	57-14-7	1,1-Dimethylhydrazine	[Elts et al. 2012]	4 L.J. Centers & 3 Charges
C2HCl3.pm	79-01-6	Trichloroethylene	[Stoll et al. 2003]	2 L.J. Centers & 1 Quadrupole

Continued on next page

Filename	CAS number	Name	Publication	Model Type
C2N2.pm	460-19-5	Cyanogen	[Miroshnichenko et al. 2013]	4 L.J. Centers & 1 Quadrupole
C3H4.pm	463-49-0	Propadiene	[Vrabec et al. 2001]	2 L.J. Centers & 1 Quadrupole
C3H6_a.pm	115-07-1	Propylene	[Vrabec et al. 2001]	2 L.J. Centers & 1 Quadrupole
C3H6_b.pm	75-19-4	Cyclopropane	[Munoz-Munoz et al. 2015]	3 L.J. Centers
C4F10.pm	355-25-9	Perfluorobutane	[Köster et al. 2012]	14 L.J. Centers & 14 Charges
C4H10.pm	75-28-5	Isobutane	[Eckl et al. 2008c]	4 L.J. Centers & 1 Dipole & 1 Quadrupole
C4H4S_I.pm	110-02-1	Thiophene	[Eckl et al. 2008c]	5 L.J. Centers & 1 Dipole & 1 Quadrupole
C4H8.pm	287-23-0	Cyclobutane	[Munoz-Munoz et al. 2015]	4 L.J. Centers
C5H10_dfg.pm	287-92-3	Cyclopentane	[Munoz-Munoz et al. 2015]	5 L.J. Centers
C5H10_diff.pm	287-92-3	Cyclopentane	[Munoz-Munoz et al. 2015]	5 L.J. Centers
C6H10O.pm	108-94-1	Cyclohexanone	[Merker et al. 2012]	7 L.J. Centers & 1 Dipole
C6H12_dfg.pm	110-82-7	Cyclohexane	[Munoz-Munoz et al. 2015]	6 L.J. Centers
C6H12_diff.pm	110-82-7	Cyclohexane	[Munoz-Munoz et al. 2015]	6 L.J. Centers
C6H12_I.pm	110-82-7	Cyclohexane	[Eckl et al. 2008c]	6 L.J. Centers & 1 Quadrupole
C6H12_II.pm	110-82-7	Cyclohexane	[Merker et al. 2012]	6 L.J. Centers
C6H12O_II.pm	108-93-0	Cyclohexanol	[Merker et al. 2009]	7 L.J. Centers & 3 Charges 1 Quadrupole
C6H4Cl2.pm	95-50-1	ortho-Dichlorobenzene	[Huang et al. 2011]	8 L.J. Centers & 1 Dipole & 4 Quadrupoles
C6H5Cl.pm	108-90-7	Chlorobenzene	[Huang et al. 2011]	7 L.J. Centers & 1 Dipole & 5 Quadrupoles
C6H6_I.pm	71-43-2	Benzene	[Guevara-Carrion et al. 2016]	6 L.J. Centers & 6 Quadrupoles
C6H6_II.pm	71-43-2	Benzene	[Huang et al. 2011]	6 L.J. Centers & 6 Quadrupoles
C7H8_I.pm	108-88-3	Toluene	[Guevara-Carrion et al. 2016]	7 L.J. Centers & 6 Quadrupoles
C7H8_II.pm	108-88-3	Toluene	[Huang et al. 2011]	7 L.J. Centers & 1 Dipole & 5 Quadrupoles
Ca2+.pm	17787-72-3	Calcium ion (2+)	[Deublein et al. 2012]	1 L.J. Center & 1 Charge
CBr2F2.pm	75-61-6	Dibromodifluoromethane	[Stoll et al. 2003]	2 L.J. Centers & 1 Dipole
CBrCl3.pm	75-62-7	Bromotrichloromethane	[Stoll et al. 2003]	2 L.J. Centers & 1 Dipole
CBrClF2.pm	353-59-3	Bromochlorodifluoromethane	[Stoll et al. 2003]	2 L.J. Centers & 1 Dipole
CC2HBrClF3.pm	151-67-7	Halothane	[Stoll et al. 2003]	2 L.J. Centers & 1 Dipole
CCl2O.pm	75-44-5	Phosgene	[Huang et al. 2011]	4 L.J. Centers & 1 Dipole & 1 Quadrupole
CCl4_I.pm	56-23-5	Carbon tetrachloride	[Vrabec et al. 2001]	2 L.J. Centers & 1 Quadrupole
CCl4_II.pm	56-23-5	Carbon tetrachloride	[Guevara-Carrion et al. 2016]	5 L.J. Centers & 5 Charges
CClN.pm	506-77-4	Cyanogen chloride	[Miroshnichenko et al. 2013]	3 L.J. Centers & 1 Quadrupole & 1 Dipole
CF2CFBr.pm	598-73-2	Bromotrifluoroethylene	[Stoll et al. 2003]	2 L.J. Centers & 1 Dipole
CF4_II.pm	75-73-0	Tetrafluoromethane	[Vrabec et al. 2001]	2 L.J. Centers & 1 Quadrupole
CH2Br2_D.pm	74-95-3	Dibromomethane	[Stoll et al. 2003]	1 L.J. Center & 1 Dipole
CH2Br2_Q.pm	74-95-3	Dibromomethane	[Stoll et al. 2003]	2 L.J. Centers & 1 Quadrupole
CH2BrCl.pm	74-97-5	Bromochloromethane	[Stoll et al. 2003]	2 L.J. Centers & 1 Dipole
CH2Cl2.pm	75-09-2	Methylene chloride	[Stoll et al. 2003]	1 L.J. Center & 1 Dipole

Continued on next page

Filename	CAS number	Name	Publication	Model Type
CH2I2.pm	75-11-6	Methylene iodide	[Stoll et al. 2003]	1 L.J. Center & 1 Dipole
CH2O.pm	50-00-0	Formaldehyde	[Eckl et al. 2008c]	2 L.J. Centers & 1 Dipole
CH2O2.pm	64-18-6	Formic acid	[Schnabel et al. 2007b]	3 L.J. Centers & 4 Charges
CH3Br.pm	74-83-9	Methyl bromide	[Stoll et al. 2003]	2 L.J. Centers & 1 Dipole
CH3Cl.pm	74-87-3	Methyl chloride	[Stoll et al. 2003]	2 L.J. Centers & 1 Dipole
CH3I.pm	74-88-4	Methyl iodide	[Stoll et al. 2003]	2 L.J. Centers & 1 Dipole
CH3NO2.pm	75-52-5	Nitromethane	[Eckl et al. 2008c]	4 L.J. Centers & 1 Dipole & 1 Quadrupole
CH3OCH3.pm	115-10-6	Dimethyl ether	[Eckl et al. 2008c]	3 L.J. Centers & 1 Dipole
CH4.pm	74-82-8	Methane	[Vrabec et al. 2001]	1 L.J. Center
CH4O_I.pm	67-56-1	Methyl alcohol	[Schnabel et al. 2007a]	2 L.J. Centers & 3 Charges
CH5N.pm	74-89-5	Methylamine	[Schnabel et al. 2008]	2 L.J. Centers & 2 Charges
CH6N2.pm	60-34-4	Methylhydrazine	[Elts et al. 2012]	3 L.J. Centers & 3 Charges
CHBr3.pm	75-25-2	Bromoform	[Stoll et al. 2003]	2 L.J. Centers & 1 Dipole
CHCCH3_I.pm	74-99-7	1-Propyne	[Vrabec et al. 2001]	2 L.J. Centers & 1 Quadrupole
CHCCH3_II.pm	74-99-7	1-Propyne	[Stoll 2004]	2 L.J. Centers & 1 Quadrupole
CHCl2F.pm	75-43-4	Dichlorofluoromethane	[Stoll et al. 2003]	2 L.J. Centers & 1 Dipole
CHCl3.pm	67-66-3	Chloroform	[Stoll et al. 2003]	2 L.J. Centers & 1 Dipole
CHN.pm	74-90-8	Hydrogen cyanide	[Eckl et al. 2008c]	2 L.J. Centers & 1 Dipole & 1 Quadrupole
Cl-_I.pm	16887-00-6	Chlorine ion (1-)	[Deublein et al. 2012]	1 L.J. Center & 1 Charge
Cl-_II.pm	16887-00-6	Chlorine ion (1-)	[Deublein et al. 2012]	1 L.J. Center & 1 Charge
Cl2.pm	7782-50-5	Chlorine	[Vrabec et al. 2001]	2 L.J. Centers & 1 Quadrupole
CO_D.pm	630-08-0	Carbon monoxide	[Stoll et al. 2003]	2 L.J. Centers & 1 Dipole
CO_Q.pm	630-08-0	Carbon monoxide	[Stoll 2004]	2 L.J. Centers & 1 Quadrupole
CO2_I.pm	124-38-9	Carbon dioxide	[Merker et al. 2010]	3 L.J. Centers & 1 Quattropole
CO2_II.pm	124-38-9	Carbon dioxide	[Stoll 2004]	2 L.J. Centers & 1 Quadrupole
Cs+.pm	18459-37-5	Cesium ion (1+)	[Deublein et al. 2012]	1 L.J. Center & 1 Charge
CS2.pm	75-15-0	Carbon disulfide	[Vrabec et al. 2001]	2 L.J. Centers & 1 Quadrupole
F-_I.pm	16984-48-8	Fluorine ion (1-)	[Deublein et al. 2012]	1 L.J. Center & 1 Charge
F-_II.pm	16984-48-8	Fluorine ion (1-)	[Deublein et al. 2012]	1 L.J. Center & 1 Charge
F2.pm	7782-41-4	Fluorine	[Vrabec et al. 2001]	2 L.J. Centers & 1 Quadrupole
NH3_II.pm	7664-41-7	Ammonia	[Eckl et al. 2008a]	1 L.J. Center & 4 Charges
H4N2.pm	302-01-2	Hydrazine	[Elts et al. 2012]	2 L.J. Centers & 6 Charges
HCl.pm	7647-01-0	Hydrochloric acid	[Huang et al. 2011]	1 L.J. Center & 2 Charges
I-_I.pm	20461-54-5	Iodide ion (1-)	[Deublein et al. 2012]	1 L.J. Center & 1 Charge
I-_II.pm	20461-54-5	Iodide ion (1-)	[Deublein et al. 2012]	1 L.J. Center & 1 Charge
I2.pm	7553-56-2	Iodine	[Vrabec et al. 2001]	2 L.J. Centers & 1 Quadrupole
K+.pm	24203-36-9	Potassium ion (1+)	[Deublein et al. 2012]	1 L.J. Center & 1 Charge

Continued on next page

Filename	CAS number	Name	Publication	Model Type
Kr.pm	7439-90-9	Krypton	[Vrabec et al. 2001]	1 L.J. Center
Li+.pm	17341-24-1	Lithium ion (1+)	[Deublein et al. 2012]	1 L.J. Center & 1 Charge
Mg2+.pm	22537-22-0	Magnesium ion (2+)	[Deublein et al. 2012]	1 L.J. Center & 1 Charge
N2.pm	7727-37-9	Nitrogen	[Stoll 2004]	2 L.J. Centers & 1 Quadrupole
Na+_I.pm	17341-25-2	Sodium ion (1+)	[Deublein et al. 2012]	1 L.J. Center & 1 Charge
Ne.pm	7440-01-9	Neon	[Vrabec et al. 2001]	1 L.J. Center
O2.pm	7782-44-7	Oxygen	[Stoll 2004]	2 L.J. Centers & 1 Quadrupole
R11_CFC13.pm	75-69-4	Trichloromonofluoromethane	[Stoll et al. 2003]	2 L.J. Centers & 1 Dipole
R1122_CHCl=CF2.pm	359-10-4	2-Chloro-1,1-difluoroethylene	[Stoll et al. 2003]	2 L.J. Centers & 1 Dipole
R112a_CCl3-CF2Cl.pm	76-11-9	1,1,1,2-Tetrachloro-2,2-difluoroethane	[Stoll et al. 2003]	2 L.J. Centers & 1 Dipole
R113_CFC12-CF2Cl.pm	76-13-1	1,1,2-trichloro-1,2,2-trifluoro-Ethane	[Stoll et al. 2003]	2 L.J. Centers & 1 Quadrupole
R114_CF2Cl-CF2Cl.pm	76-14-2	1,2-dichloro-1,1,2,2-tetrafluoro-Ethane	[Stoll et al. 2003]	2 L.J. Centers & 1 Quadrupole
R115_CF3-CF2Cl.pm	76-15-3	Pentafluoroethyl chloride	[Stoll et al. 2003]	2 L.J. Centers & 1 Quadrupole
R12_CF2Cl2.pm	75-71-8	Dichlorodifluoromethane	[Stoll et al. 2003]	2 L.J. Centers & 1 Dipole
R123_CHCl2-CF3.pm	306-83-2	2,2-dichloro-1,1,1-trifluoro-Ethane	[Stoll et al. 2003]	2 L.J. Centers & 1 Dipole
R124_CHFCl-CF3.pm	2837-89-0	2-chloro-1,1,1,2-tetrafluoro-Ethane	[Stoll et al. 2003]	2 L.J. Centers & 1 Dipole
R125_CHF2-CF3.pm	354-33-6	pentafluoro-Ethane	[Stoll et al. 2003]	2 L.J. Centers & 1 Dipole
R13_CF3Cl.pm	75-72-9	Chlorotrifluoromethane	[Stoll et al. 2003]	2 L.J. Centers & 1 Dipole
R134_CHF2-CHF2.pm	359-35-3	1,1,2,2-tetrafluoro-Ethane	[Stoll et al. 2003]	2 L.J. Centers & 1 Quadrupole
R134a_CH2F-CF3.pm	811-97-2	Norflurane	[Stoll et al. 2003]	2 L.J. Centers & 1 Dipole
R13B1_CBrF3.pm	75-63-8	Bromotrifluoromethane	[Stoll et al. 2003]	2 L.J. Centers & 1 Dipole
R141b_CH3-CFCl2.pm	1717-00-6	1,1-Dichloro-1-fluoroethane	[Stoll et al. 2003]	2 L.J. Centers & 1 Dipole
R142b_CH3-CF2Cl.pm	75-68-3	1-chloro-1,1-difluoro-Ethane	[Stoll et al. 2003]	2 L.J. Centers & 1 Dipole
R143a_CH3-CF3.pm	420-46-2	1,1,1-trifluoro-Ethane	[Stoll et al. 2003]	2 L.J. Centers & 1 Dipole
R152a_CH3-CHF2.pm	75-37-6	1,1-difluoro-Ethane	[Stoll et al. 2003]	2 L.J. Centers & 1 Dipole
R22_CHF2Cl.pm	75-45-6	Difluorochloromethane	[Stoll et al. 2003]	2 L.J. Centers & 1 Dipole
R227ea_C3HF7.pm	431-89-0	1,1,1,2,3,3,3-heptafluoro-Propane	[Eckl et al. 2007]	10 L.J. Centers & 1 Dipole 1 Quadrupole
R23_CHF3.pm	75-46-7	Fluoroform	[Stoll et al. 2003]	2 L.J. Centers & 1 Dipole
R32_CH2F2.pm	75-10-5	Difluoromethane	[Stoll et al. 2003]	1 L.J. Center & 1 Dipole
R41_CH3F.pm	593-53-3	Methyl fluoride	[Stoll et al. 2003]	2 L.J. Centers & 1 Dipole
Rb+.pm	22537-38-8	Rubidium ion (1+)	[Deublein et al. 2012]	1 L.J. Center & 1 Charge
SF6.pm	2551-62-4	Sulfur hexafluoride	[Vrabec et al. 2001]	2 L.J. Centers & 1 Quadrupole
SO2.pm	7446-09-5	Sulfur dioxide	[Eckl et al. 2008c]	3 L.J. Centers & 1 Dipole & 1 Quadrupole
Sr.pm	22537-39-9	Strontium ion (2+)	[Deublein et al. 2012]	1 L.J. Center & 1 Charge
Xe.pm	7440-63-3	Xenon	[Vrabec et al. 2001]	1 L.J. Center

Bibliography

- Deublein, S., J. Vrabec, and H. Hasse (2012). “A set of molecular models for alkali and halide ions in aqueous solution”. In: *The Journal of Chemical Physics* (cit. on pp. 2, 4, 5).
- Deublein, S., S. Reiser, J. Vrabec, and H. Hasse (2012). “A Set of Molecular Models for Alkaline-Earth Cations in Aqueous Solution”. In: *Journal of Physical Chemistry B* 116.18, p. 5448. DOI: 10.1021/jp3013514 (cit. on pp. 2–5).
- Deublein, S., P. Metzler, J. Vrabec, and H. Hasse (2013). “Automated development of force fields for the calculation of thermodynamic properties acetonitrile as a case study”. In: *Molecular Simulation* 39.2, p. 109. DOI: 10.1080/08927022.2012.705434 (cit. on p. 2).
- Eckl, B., Y. Huang, and H. Vrabec J.and Hasse (2007). “Vapor pressure of R227ea + ethanol at 343.13K by molecular simulation”. In: *Fluid Phase Equilibria* 260, 177–182. DOI: 10.1016/j.fluid.2007.05.011 (cit. on p. 5).
- Eckl, B., J. Vrabec, and H. Hasse (2008a). “An optimised molecular model for ammonia”. In: *Molecular Physics: An International Journal at the Interface Between Chemistry and Physics* 106.8, p. 1039. DOI: 10.1080/00268970802112137 (cit. on p. 4).
- Eckl, B., J. Vrabec, and H. Hasse (2008b). “On the application of force fields for predicting a wide variety of properties: Ethylene oxide as an example”. In: *Fluid Phase Equilibria* 274.1. DOI: 10.1016/j.fluid.2008.02.002 (cit. on p. 2).
- Eckl, B., J. Vrabec, and H. Hasse (2008c). “Set of Molecular Models Based on Quantum Mechanical Ab Initio Calculations and Thermodynamic Data”. In: *The Journal of Physical Chemistry B* (cit. on pp. 2–5).
- Eltz, E., T. Windmann, D. Staak, and J. Vrabec (2012). “Fluid phase behavior from molecular simulation Hydrazine, Monomethylhydrazine, Dimethylhydrazine and binary mixtures containing these compounds”. In: *Fluid Phase Equilibria* 322. DOI: 10.1016/j.fluid.2012.03.008 (cit. on pp. 2, 4).
- Guevara-Carrion, G., T. Janzen, Y. Munoz-Munoz, and J. Vrabec (2016). “Mutual diffusion of binary liquid mixtures containing methanol, ethanol, acetone, benzene, cyclohexane, toluene, and carbon tetrachloride”. In: *The Journal of Chemical Physics* 144. DOI: 10.1063/1.4943395. URL: <http://dx.doi.org/10.1063/1.4943395> (cit. on p. 3).
- Huang, Y., M. Heilig, J. Vrabec, and H. Hasse (2011). “Vapor-Liquid Equilibria of Hydrogen Chloride, Phosgene, Benzene, Chlorobenzene, Ortho-Dichlorobenzene and Toluene by Molecular Simulation”. In: *AIChE Journal* 57.4, p. 1043. DOI: 10.1002/aic.12329 (cit. on pp. 3, 4).
- Huang Y. aHuang, Y. T., M. Heilig, H. Hasse, and J. Vrabec (2012). “Molecular Modeling and Simulation of Vapor–Liquid Equilibria of Ethylene Oxide, Ethylene Glycol, and Water as Well as their Binary Mixtures”. In: *Ind. Eng. Chem. Res.* 51.21. DOI: 10.1021/ie300248z (cit. on p. 2).

- Köster, A., P. Nandi, T. Windmann, D. Ramjugernath, and J. Vrabec (2012). “Vapor–liquid equilibria of ethylene (C₂H₄) + decafluorobutane (C₄F₁₀) at 268–298 K from experiment, molecular simulation and the Peng–Robinson equation of state”. In: *Fluid Phase Equilibria* 336. DOI: 10.1016/j.fluid.2012.08.023 (cit. on p. 3).
- Merker, T., J. Vrabec, and H. Hasse (2012). “Molecular simulation study on the solubility of carbon dioxide in mixtures of cyclohexane + cyclohexanone”. In: *Fluid Phase Equilibria* 315, p. 77. DOI: 10.1016/j.fluid.2011.11.003 (cit. on p. 3).
- Merker, T., G. Guevara-Carrion, J. Vrabec, and H. Hasse (2009). *HIGH PERFORMANCE COMPUTING IN SCIENCE AND ENGINEERING '08*. Ed. by W. E. Nagel, D. B. Kroner, and M. M. Resch. Springer. DOI: 10.1007/978-3-540-88303-6_37 (cit. on p. 3).
- Merker, T., C. Engin, J. Vrabec, and H. Hasse (2010). “Molecular model for carbon dioxide optimized to vapor-liquid equilibria”. In: *The Journal of Chemical Physics* 132, p. 234512. DOI: 10.1063/1.3434530 (cit. on p. 4).
- Miroshnichenko, S., T. Grützner, D. Staak, and J. Vrabec (2013). “Molecular simulation of the vapor–liquid phase behavior of cyanides and their binary mixtures”. In: *Fluid Phase Equilibria* 354. DOI: 10.1016/j.fluid.2013.06.039 (cit. on p. 3).
- Munoz-Munoz, Y.M., G. Guevara-Carrion, M. Llano-Restrepo, and J. Vrabec (2015). “Lennard-Jones force field parameters for cyclic alkanes from cyclopropane to cyclohexane”. In: *Fluid Phase Equilibria* 404, p. 150. DOI: 10.1016/j.fluid.2015.06.033 (cit. on p. 3).
- Schnabel, T., J. Vrabec, and H. Hasse (2005). “Henry’s law constants of methane, nitrogen, oxygen and carbon dioxide in ethanol from 273 to 498 K: Prediction from molecular simulation”. In: *Fluid Phase Equilibria* 233, pp. 134–143. DOI: 10.1016/j.fluid.2005.04.016 (cit. on p. 2).
- Schnabel, T., J. Vrabec, and H. Hasse (2008). “Molecular simulation study of hydrogen bonding mixtures and new molecular models for mono- and dimethylamine”. In: *Fluid Phase Equilibria* 263, 144–159. DOI: 10.1016/j.fluid.2007.10.003 (cit. on p. 4).
- Schnabel, T., A. Srivastava, J. Vrabec, and H. Hasse (2007a). “Hydrogen Bonding of Methanol in Supercritical CO₂: Comparison between 1H NMR Spectroscopic Data and Molecular Simulation Results”. In: *J.Phys.Chem. B* 111.33, p. 9871. DOI: 10.1021/jp0720338 (cit. on p. 4).
- Schnabel, T., M. Cortada, J. S. Vrabec J.Vrabec, and H. Hasse (2007b). “Molecular model for formic acid adjusted to vapor–liquid equilibria”. In: *Chemical Physics Letters* 435.4, p. 268. DOI: 10.1016/j.cplett.2006.12.091 (cit. on p. 4).
- Stoll, J. (2004). “Molecular Models for the Prediction of Thermophysical Properties of Pure Fluids and Mixtures”. PhD thesis. Universität Stuttgart (cit. on pp. 2, 4, 5).
- Stoll, J., J. Vrabec, and H. Hasse (2003). “A set of molecular models for carbon monoxide and halogenated hydrocarbons”. In: *The Journal of Chemical Physics* 119, p. 11396. DOI: 10.1063/1.1623475 (cit. on pp. 2–5).
- Vrabec, J., J. Stoll, and H. Hasse (2001). “A Set of Molecular Models for Symmetric Quadrupolar Fluids”. In: *The Journal of Physical Chemistry B* 105.48, p. 12126. DOI: 10.1021/jp012542o (cit. on pp. 2–5).